Published in final edited form as:
Cell. 2009 July 23; 138(2): 245–256. doi:10.1016/j.cell.2009.04.056.

Androgen Receptor Regulates a Distinct Transcription Program in Androgen-Independent Prostate Cancer

Qianben Wang[1,2,*,14], **Wei Li**[3,14], **Yong Zhang**[4], **Xin Yuan**[5], **Kexin Xu**[1], **Jindan Yu**[6], **Zhong Chen**[2], **Rameen Beroukhim**[1,7], **Hongyun Wang**[5], **Mathieu Lupien**[1,13], **Tao Wu**[8], **Meredith M. Regan**[4], **Clifford A. Meyer**[4], **Jason S. Carroll**[9], **Arjun Kumar Manrai**[4], **Olli A. Jänne**[10], **Steven P. Balk**[5], **Rohit Mehra**[6], **Bo Han**[6], **Arul M. Chinnaiyan**[6], **Mark A. Rubin**[11], **Lawrence True**[12], **Michelangelo Fiorentino**[1], **Christopher Fiore**[1], **Massimo Loda**[1], **Philip W. Kantoff**[1], **X. Shirley Liu**[4,*], and **Myles Brown**[1,*]

[1] Department of Medical Oncology, Dana-Farber Cancer Institute and Harvard Medical School, Boston, MA 02115, USA [2] Department of Molecular and Cellular Biochemistry and the Comprehensive Cancer Center, Ohio State University College of Medicine, Columbus, OH 43210, USA [3] Division of Biostatistics, Dan L. Duncan Cancer Center and Department of Molecular and Cellular Biology, Baylor College of Medicine, Houston, TX 77030, USA [4] Department of Biostatistics and Computational Biology, Dana-Farber Cancer Institute and Harvard School of Public Health, Boston, MA 02115, USA [5] Cancer Biology Program, Hematology-Oncology Division, Department of Medicine, Beth Israel Deaconess Medical Center and Harvard Medical School, Boston, MA 02215, USA [6] Department of Pathology, University of Michigan Medical School, Ann Arbor, MI 48109, USA [7] Broad Institute of Harvard and MIT, Cambridge, MA 02139, USA [8] Department of System Biology, Harvard Medical School, Boston, MA 02115, USA [9] Cancer Research UK, Cambridge Research Institute, Robinson Way, Cambridge CB20RE, UK [10] Biomedicum Helsinki, Institute of Biomedicine (Physiology), University of Helsinki, Helsinki, FI-00014, Finland [11] Department of Pathology and Laboratory Medicine, Weill Cornell Medical College, New York, NY 10021, USA [12] Department of Pathology, University of Washington Medical Center, Seattle, WA 98195, USA

SUMMARY

The evolution of prostate cancer from an androgen-dependent state (ADPCa) to one that is androgen-independent (AIPCa) marks its lethal progression. The androgen receptor (AR) is essential in both, though its function in AIPCa is poorly understood. We have defined the direct AR-dependent target genes in both AIPCa and ADPCa by generating AR-dependent gene expression profiles and AR cistromes. In contrast to ADPCa, AR selectively up-regulates M-phase cell cycle genes in AIPCa including *UBE2C*, a gene that inactivates the M-phase checkpoint. Selective epigenetic marks and collaborating transcription factor occupancy at UBE2C enhancers leads to increased AR recruitment and UBE2C over-expression in AIPCa cell lines and clinical cases. Silencing of UBE2C blocks AIPCa but not ADPCa growth. Thus the role of AR in AIPCa is not to direct the androgen-dependent gene expression program without androgen, but rather to execute a distinct program resulting in androgen-independent growth.

*Correspondence: qianben.wang@osumc.edu (Q.W.), xsliu@jimmy.harvard.edu (X.S.L.), myles__brown@dfci.harvard.edu (M.B.).
[13]Present address: Department of Genetics, Norris Cotton Cancer Center, Dartmouth Medical School, Lebanon, NH 03756, USA.
[14]These authors contributed equally to this work

INTRODUCTION

Androgens, functioning through the androgen receptor (AR), are essential for the initiation and progression of prostate cancer (Heinlein and Chang, 2004). Thus androgen-ablation therapies, which involve surgical castration or the use of luteinizing hormone-releasing hormone (LHRH) agonists (or antagonists), have been the mainstay of treatment for advanced ADPCa for over 40 years. While such therapies initially lead to disease regression, in general advanced prostate cancer ultimately progresses to an androgen-independent late stage that is refractory to current therapies (also termed "castration-resistant prostate cancer") (Debes and Tindall, 2004; Feldman and Feldman, 2001). As AR is expressed in the vast majority of both ADPCa and AIPCa (Heinlein and Chang, 2004; Scher and Sawyers, 2005) and decreasing levels of AR protein expression reduces both ADPCa and AIPCa growth in model systems (Chen et al., 2004; Haag et al., 2005; Heinlein and Chang, 2004), it appears AR signaling pathways play a critical role in both ADPCa and AIPCa.

AR is a member of nuclear hormone receptor superfamily that regulates target gene expression in a ligand-inducible manner (Mangelsdorf et al., 1995). Two well-characterized AR target genes in ADPCa are prostate specific antigen (PSA) and the TMPRSS2-ETS fusion genes. Recent studies have demonstrated that control of these target genes involves long-range, combinatorial regulation by AR, DNA-binding collaborating transcription factors and non-DNA binding co-regulatory factors (Shang et al., 2002; Wang et al., 2005; Wang et al., 2007). While the role of AR target genes in regulating cell cycle progression in ADPCa have yet to be fully defined, it is well understood that decreased ADPCa growth after AR silencing and/or androgen deprivation primarily involves a block of the G1/S cell cycle transition through AR-dependent regulation of cyclin D1, p21 and p27 (Comstock and Knudsen, 2007). In contrast, how AR regulates cell growth in AIPCa is not known. Addressing this question is of clinical importance as it may lead to the identification of specific therapeutic targets for this lethal stage of the disease. By comparing the program of gene expression directly regulated by AR in a model of the progression of ADPCa to AIPCa and gene and protein expression from actual AIPCa cases we find that AR selectively and directly up-regulates a set of M-phase cell cycle genes to promote AIPCa growth.

RESULTS

M-phase cell cycle genes are up-regulated genes both in a cell culture model of AIPCa and in clinical AIPCa samples

To mimic the properties of clinical prostate cancer progression, we utilized LNCaP-abl (abl), an androgen-independent derivative of the androgen-dependent LNCaP prostate cancer cell line that was generated after long-term androgen deprivation (Culig et al., 1999). Consistent with its AIPCa phenotype abl cells grow substantially more rapidly than LNCaP cells in hormone-depleted medium (Figure S1). While the physiological androgen 5α-dihydrotestosterone (DHT) significantly increases LNCaP cell proliferation, it has little effect on abl cell growth (Figure S1A). To identify genes that might account for the androgen-independent growth of abl compared with LNCaP, we examined gene expression profiles of abl cells in the absence of DHT and LNCaP cells in the absence and presence of DHT treatment for 4 hr (Figure S1B). Gene Ontology (GO) analysis of up-regulated transcripts in abl compared with LNCaP in the absence of DHT showed that the top two enriched GO biological processes are "cell cycle" ($p=2.8 \times 10^{-19}$, modified Fisher exact p value, hereinafter) and "mitotic cell cycle" ($p=2.2 \times 10^{-17}$), suggesting that higher expression of cell cycle genes, particularly M-phase genes, may contribute to AIPCa growth. Interestingly, GO analysis of up-regulated transcripts in abl compared with LNCaP cells treated with DHT for 4 hr also revealed that "M phase" ($p=8.8 \times 10^{-22}$) and "Cell cycle" ($p=1.4 \times 10^{-21}$) as top two enriched GO biological

processes, suggesting that androgen does not directly increase cell cycle gene transcription in LNCaP cells to promote their growth. This result is consistent with a recent study demonstrating that androgen induces LNCaP growth through mTOR activation and a post-transcriptional increase in Cyclin D protein level (Xu et al., 2006). We next investigated whether cell cycles genes are also enriched in up-regulated genes from clinical cases of AIPCa compared with ADPCa cases. This was accomplished by re-analyzing gene expression profiles of AIPCa and ADPCa from two clinical studies (Figure S1B) (Stanbrough et al., 2006; Varambally et al., 2005). In agreement with the cell line results, the most significantly enriched GO biological processes categories in clinical AIPCa up-regulated transcripts are also "cell cycle" (Varambally dataset, $p=4.7 \times 10^{-15}$, and Stanbrough dataset, $p=2.7 \times 10^{-23}$) and "mitotic cell cycle" (Varambally dataset, $p=6.3 \times 10^{-16}$, and Stanbrough dataset, $p=1.9 \times 10^{-22}$). These data demonstrate that expression of cell cycle regulatory genes, primarily M-phase genes are enriched in AIPCa and may promote AIPCa growth.

AR up-regulates M-phase cell cycle genes to promote AIPCa growth

Given our finding that expression of specific cell cycle genes are up-regulated in abl compared with LNCaP and the requirement of AR for growth of both cell lines (Figure 1A), we hypothesized that AR promotes AIPCa proliferation by up-regulating specific cell cycle genes. We next performed gene expression profiling to define AR-dependent genes in abl by transfection of a short interfering RNA (siRNA) against AR (siAR) or a control siRNA (siControl). As referents, we also performed gene expression analysis in LNCaP cells following AR silencing and in both cell lines over a time course of DHT stimulation (0, 4 hr, and 16 hr) (Figure 1B)(Wang et al., 2007). Unsupervised hierarchical clustering of the expression data clearly distinguished androgen-regulated genes and AR-regulated genes that reflect ligand-activated and basal AR activity, respectively (Figure 1B). Therefore, AR-regulated genes in AIPCa are not the same as those regulated by androgen in ADPCa (Figures 1C and S2). As AR silencing decreases abl cell proliferation (Figure 1A), we next focused on the AR up-regulated genes in abl cells (i.e. siControl/siAR up-regulated genes). Interestingly, GO analysis of 345 abl-specific AR up-regulated transcripts ($q < 0.05$) (Figure 1C) revealed that "cell cycle" (52 transcripts, $p=1.4 \times 10^{-9}$) and "mitotic cell cycle" (24 transcripts, $p=8.0 \times 10^{-9}$) are the top two over-represented GO biological processes. Moreover, comparing these AR up-regulated cell cycle transcripts in abl cells with up-regulated transcripts in clinical AIPCa showed very significant overlaps (hypergeometric distribution, for cell cycle transcripts: 36% ($p=8.85 \times 10^{-3}$) overlap with Varambally dataset and 50.9% ($p=1.05 \times 10^{-3}$) overlap with Stanbrough dataset; for M phase transcripts: 62.5% ($p=1.20 \times 10^{-5}$) overlap with Varambally dataset and 91.7% ($p=4.02 \times 10^{-10}$) overlap with Stanbrough dataset) (Figure 1D). In contrast to enriched "cell cycle" and "mitotic cell cycle" GO biological processes for abl-specific AR up-regulated transcripts, the most significantly enriched GO biological processes for 23 LNCaP-specific basal AR up-regulated transcripts and 435 LNCaP-specific transcripts up-regulated by 4 hr DHT treatment (Figure 1C) are "cellular lipid metabolism" ($p=7.7 \times 10^{-2}$) and "positive regulation of cellular process ($p=9.7 \times 10^{-}5$)", respectively. In addition, 291 of 345 transcripts abl-specific AR up-regulated transcripts ($q<0.05$) have a higher AR induced gene expression fold change in abl than in LNCaP cells. GO analysis of these 291 genes also revealed that "cell cycle" ($p=2.6 \times 10^{-9}$) and "mitotic cell cycle" ($p=5.2 \times 10^{-9}$) as the top two enriched GO biological processes. Taken together these data suggest that AR selectively up-regulates M-phase cell cycle genes to promote AIPCa growth.

Preferential AR binding to the M-phase genes leads to higher expression in AIPCa

To investigate the underlying regulatory mechanism for the differential pattern of AR-regulated genes in AIPCa and ADPCa, we defined the AR cistrome by combining chromatin immunoprecipitation (ChIP) with tiled oligonucleotide microarrays across the entire human genome (ChIP-on-chip) in abl and LNCaP cells. In order to increase the sensitivity of our

approach (Johnson et al., 2008), we performed the AR ChIP-on-chip in the presence of DHT in both cell lines. Our strategy is to identify AR binding sites by ChIP-on-chip in the presence of androgen followed by the validation of sites of interest by directed ChIP in both the presence and absence of androgen. Using the MAT algorithm (Johnson et al., 2006), we identified 8,708 AR binding sites in LNCaP cells and 6,353 AR binding regions in abl cells based on a stringent false discovery rate (FDR) of 5% (Figure S3). As positive controls, we found that these included previously reported AR binding regions at the *PSA, KLK2* and *TMPRSS2* genes (Figure S4) (Schuur et al., 1996; Sun et al., 1997; Wang et al., 2007; Yu et al., 1999). We next compared AR binding in two cell lines using a less stringent statistical cutoff ($p < 1\times10^{-4}$ or FDR 15%) to avoid missing true differential binding sites with low binding affinity (MAT score). LNCaP cells have a greater number of higher affinity AR binding sites than do abl cells (Figures 2A and S5), which is consistent with a previous report showing that androgen signaling activity is significantly decreased in AIPCa compared with ADPCa (Tomlins et al., 2007). Correlation of AR binding sites with activated and basal AR-regulated genes showed a significant enrichment of AR binding within 20–50 kb of the transcription start sites (TSS) of up-regulated genes but not of down-regulated genes in both ADPCa and AIPCa (Figures 2B and S6), suggesting that these up-regulated genes are primarily direct targets of AR action.

Although in general the level AR occupancy at target sites is greater in LNCaP cells than in abl cells (Figure 3A), we find greater occupancy of AR binding near abl-specific AR up-regulated cell cycle genes and M-phase genes in abl cells than in LNCaP cells (Figure 3A and Table S2). Greater levels of AR binding are correlated with higher expression of target cell cycle and M-phase genes in abl (Figure 3B and Table S2). Directed ChIP for the AR binding sites near the M phase cell cycle regulatory genes *CDC20*, *UBE2C*, *CDK1*, and *ANAPC10* confirmed that these sites are preferentially occupied in abl as compared with LNCaP in the presence of DHT and have significant AR occupancy in the absence of hormone only in abl and not in LNCaP (Figure 3C). We examined the mRNA (Figure 3D) and protein (Figure 3E) expression of *CDC20*, *UBE2C*, and *CDK1* in abl and LNCaP cells in the absence of hormone and following AR silencing. These results confirmed that these genes are differentially up-regulated and AR-dependent in abl as compared with LNCaP.

Selective active epigenetic marks and collaborating transcription factors at M-phase gene enhancers lead to increased AR occupancy at these sites in AIPCa

Among the specific AR regulated M-phase cell cycle genes in abl cells, ubiquitin-conjugating enzyme E2C (UBE2C), an anaphase-promoting complex (APC)-specific ubiquitin-conjugating enzyme, is of particular interest as the expression of this gene was recently found to be critical for inactivating the cell cycle M-phase checkpoint (Reddy et al., 2007). Therefore, we further characterized the two specific UBE2C AR binding sites that are located −32.8 kb and +41.6 kb away from the TSS of *UBE2C* gene in abl cells (Figure S7). While these two putative enhancers are within or downstream of other annotated genes, *UBE2C* is the only AR dependent gene in the region. Furthermore, quantitative chromosome conformation capture assays (3C-qPCR) demonstrated significantly greater interaction between these two putative enhancers and the UBE2C promoter in abl cells than in LNCaP cells in the absence of hormone (Figure 4A). In order to determine the mechanism of the preferential occupancy of the UBE2C enhancer sequences in abl we examined whether there were abl-specific sequence alterations in these regions. Sequencing of the two UBE2C enhancer regions identified by AR ChIPon-chip in LNCaP and abl cells revealed that these two regions are 100% identical in the two cell lines (data not shown).

Given our previous findings that collaborating transcription factors and coactivators may assist nuclear receptor binding in certain regions (Carroll et al., 2005; Shao et al., 2004; Wang et al., 2007), we then investigated whether the previously identified AR collaborating factors FoxA1,

GATA2 and Oct1 (Wang et al., 2007) and AR coactivator MED1 (TRAP220) (Wang et al., 2005; Wang et al., 2002) are differentially recruited to the UBE2C enhancers in two cell lines. Directed ChIP analysis showed significantly higher occupancy of FoxA1 and MED1 to both enhancers and GATA2 to enhancer 2 in abl cells as compared with LNCaP cells (Figures 4B and 4C). We also examined serine 5 phosphorylated polymerase II (P-pol II ser 5) occupancy at the UBE2C promoter in both cell lines (Figure 4D). We find significantly greater P-pol II ser 5 occupancy at the UBE2C promoter in abl compared with LNCaP cells that is unchanged by the addition of DHT. In contrast, at the PSA promoter P-pol II ser 5 occupancy is significantly greater in LNCaP cells and is stimulated by DHT. The greater level of AR transcription complex loading on the UBE2C enhancers leads to a greater level of P-pol II ser 5 at the promoter through chromosomal looping (Figure 4A), resulting in higher UBE2C expression levels in abl cells (Figures 3D and 4E). Importantly, silencing of FoxA1, GATA2 or MED1 decreases UBE2C mRNA level in abl cells but not in LNCaP cells (Figure 4E), suggesting that each of these factors plays an indispensable role in mediating UBE2C expression.

Interestingly, while minimally greater levels MED1 protein expression in abl (Figure 4F) might account for greater MED1 recruitment to the UBE2C enhancers, differences in expression do not account for the differential recruitment of FoxA1 and GATA2 to the UBE2C enhancers. We have recently defined a role for the active enhancer histone marks H3 lysine 4 mono- and di-methyl (H3K4me1 and H3K4me2) (Bernstein et al., 2005; Heintzman et al., 2007) in specifying sites of FoxA1 recruitment in various cell types (Lupien et al., 2008), we therefore examined the levels of these marks (and as control the promoter-specific H3K4me3 mark) at the UBE2C enhancers. We find that H3K4me1 and H3K4me2 are significantly enriched at the UBE2C enhancers only in abl and not in LNCaP (Figures 4G and 4H) suggesting that these epigenetic marks may define these sites as abl-specific enhancers leading to AR-dependent expression of UBE2C only in this cell type.

In order to determine whether H3K4 methylation is required for the increased AR occupancy at the UBE2C enhancers in abl cells we over-expressed a H3K4me1 and H3K4me2 specific demethylase KDM1 (Shi et al., 2004) in both LNCaP and abl cells. Consistent with our recent finding that KDM1 over-expression reduces FoxA1 recruitment in MCF7 cells (Lupien et al., 2008), we found that KDM1 over-expression decreases FoxA1 binding and H3K4me2 level at the UBE2C enhancers (Figure S8). More significantly, over-expression of KDM1 almost completely abolishes AR binding in both cell lines (Figure 5A), suggesting that H3K4 marks are required for differential AR binding at the UBE2C enhancers in LNCaP and abl cells. Interestingly, FoxA1 silencing also almost fully abolishes AR binding at the UBE2C enhancers in LNCaP and abl cells (Figure 5B), suggesting FoxA1 binding is also essential for differential AR recruitment. By contrast, silencing of AR has no effect on differential H3K4me2 level and FoxA1 binding on the UBE2C enhancers (Figure 5C). In addition, FoxA1 silencing has no effect on differential H3K4me2 levels on the UBE2C enhancers (Figure S9). Thus the differential H3K4 marks and FoxA1 act upstream of AR and are required for differential AR binding at the UBE2C enhancers (Figure 5D).

To confirm that the requirement for H3K4 methylation and FoxA1 binding for AR binding was not restricted to the UBE2C enhancers, we performed H3K4me1, H3K4me2 and FoxA1 ChIP on the CDK1, CDC20 and ANAPC10 enhancers. We find that the levels of H3K4 methyl marks and FoxA1 are also higher on these enhancers in abl cells than LNCaP cells (Figure S10). As controls, the H3K4 marks and FoxA1 are not present at randomly selected androgen responsive elements (ARE) that have no AR binding (Figure S10). As expected, over-expression of KDM1 or silencing of FoxA1 also significantly decreases AR binding on the CDK1 and CDC20 enhancers (Figure S11). Moreover, over-expression of UBE2C does not increase AR binding at the CDK1, CDC20 and ANAPC10 enhancers in LNCaP cells (Figure

S12). These findings suggest that increased AR binding at the enhancers of other M-phase genes in abl cells is also determined by H3K4 methylation and FoxA1 binding rather than being the result of increased UBE2C expression.

Higher levels of H3K4 methylation and FoxA1 binding at the UBE2C enhancers leads to over-expression of UBE2C protein in AIPCa cases

In order to confirm that AR-dependent over-expression of UBE2C is not unique to abl cells, we determined UBE2C protein expression levels in another model of AIPCa and in clinical AIPCa cases. We confirmed that UBE2C protein level is greater and AR-dependent in the androgen-independent cell line C4-2B (Thalmann et al., 2000) than in LNCaP (Figure S13). More significantly we examined UBE2C protein expression in clinical cases of AIPCa. We measured by immunohistochemistry UBE2C protein levels in tissue microarrays containing normal prostate, ADPCa and AIPCa tissues (n=372 tissue microarray elements). AIPCa samples showed strong UBE2C staining, whereas weak and no staining was observed in ADPCa and normal prostate, respectively (Figures 6A and 6B). These data suggest that UBE2C protein over-expression correlates with the occurrence and progression of prostate cancer.

To investigate whether the over-expression of UBE2C protein in clinical samples is also caused by enhanced AR transcription complex occupancy at the UBE2C enhancers, we performed AR, FoxA1, H3K4me1 and H3K4me2 ChIP using tissues from ADPCa and AIPCa cases. We found significantly greater AR and FoxA1 occupancy and H3K4 methylation at the UBE2C enhancers in a case of AIPCa as compared with an ADPCa case (Figure S14). While limited by the number of available cases for analysis, this finding is consistent with our findings in LNCaP and abl and supports the conclusion that increased H3K4 methylation and FoxA1 and AR occupancy at the UBE2C enhancers leads to increased UBE2C expression in AIPCa.

Functional role of UBE2C in AIPCa growth

Finally, we explored the functional role of UBE2C in prostate cancer growth. Although over-expression of UBE2C in LNCaP cells is not sufficient to accelerate LNCaP cell grow in the absence of androgen (Figure S15), silencing of UBE2C selectively decreases abl (two-side t-test, $p= 9.1 \times 10^{-3}$) but not LNCaP cell proliferation (Figure 7A), suggesting that UBE2C is necessary for abl cell proliferation in the absence of hormone (Figures 7A and S1A). The UBE2C protein half-life of ~6 hr in both LNCaP and abl cells (Figure S16) suggests that it is AR-dependent androgen-independent up-regulation *UBE2C* transcription (Figures 4, 5, 6 and S14) rather than a more stable UBE2C protein that contributes to its increased level and the increased growth of abl cells in the absence of androgen.

Consistent with the critical role of UBE2C in inactivating the M-phase checkpoint (Reddy et al., 2007), fluorescence-activated cell sorting (FACS) analysis revealed that silencing of UBE2C causes a G2/M accumulation in both cell lines (Figure 7B). As previously reported, AR silencing leads to a G1/S block in LNCaP cells (Comstock and Knudsen, 2007), however it leads to a G2/M block in abl cells (Figure 7B). This increase in G2/M phase cells was further confirmed by an increase in histone H3 serine 10 phosphorylation (P-H3Ser10) level (Figure 7C) that peaks in metaphase (Prigent and Dimitrov, 2003). Interestingly, silencing of UBE2C in both LNCaP and abl cells also led to an increase S phase (Figure 7B), which could caused by either a S phase block or a shortened G1. To distinguish between these two possibilities, we synchronized siControl and siUBE2C transfected LNCaP and abl cells in G0 by serum starvation. Cells were then released into cell cycle by the addition of serum. We measured cyclin A protein level over time as this cyclin is not detected during early G1, accumulates at the end of G1 and is essential for G1/S transition (Girard et al., 1991; Resnitzky et al., 1995). Interestingly, we found that Cyclin A accumulated 2 hr earlier in siUBE2C transfected (12 hr) than in siControl transfected (14 hr) LNCaP cells (Figure 7D). In contrast, Cyclin A was

detected at the same time point (14 hr) in siUBE2C and siControl transfected abl cells (Figure 7D). These data suggest that UBE2C silencing results in a shortened G1 phase in LNCaP but not in abl cells. Thus the increased S phase fraction observed upon UBE2C silencing (Figure 6B) is likely a result of a delayed S phase in abl cells and shortened G1 phase in LNCaP cells. This may explain why silencing of UBE2C decreases abl but not LNCaP proliferation, even though UBE2C silencing results in G2/M block in both cell lines. The more significant effect CDK1 and CDC20 silencing on cell proliferation in abl cells than in LNCaP cells (Figure S17) may also be the result of a similar mechanism.

DISCUSSION

AR has been found to play a critical role in the development of both ADPCa and most cases of AIPCa (Debes and Tindall, 2004; Feldman and Feldman, 2001; Heinlein and Chang, 2004). In ADPCa, AR promotes cell proliferation through regulation of the cell cycle G1/S transition only in the presence of androgen (Comstock and Knudsen, 2007). In contrast, in AIPCa, AR is thought to remain active through a variety of potential mechanisms including AR amplification, AR mutation, increased androgen sensitivity, local androgen production and growth factor activation (Debes and Tindall, 2004; Feldman and Feldman, 2001; Heinlein and Chang, 2004). However, which of these mechanisms is operant and how the “activated” AR regulates AIPCa growth is poorly understood. In this study, using cell line models of AIPCa and gene expression data and tissue from actual AIPCa cases, we find that the program of gene expression regulated by AR in the absence of hormone is distinct from the androgen-regulated program in ADPCa.

In contrast to a differentiated prostate program regulated by androgens in LNCaP, AR regulates mitotic cell cycle genes in abl raising the question as to how this different AR-dependent program is executed in abl cells. Through an integrated analysis of AR cistrome and gene expression data, we found that up-regulated genes including cell cycle genes in abl cells are direct AR direct targets (Figure 2B). By analyzing the epigenetic marks and collaborating transcription factors present at the AR bound M-phase gene enhancers we explored the mechanisms underlying the reprogrammed AR action in both a AIPCa model system and clinical cases of AIPCa. We found levels of active H3K4 methyl marks and recruitment of other transcription factors including FoxA1 at AR target enhancers, most notably the UBE2C enhancers. Although increased H3K4 methylation may lead to increased recruitment of FoxA1 to facilitate greater AR occupancy (Figures S8 and 5), these active histone marks may also act upstream of other transcription factors and coactivators (e.g. GATA2 and MED1) or directly on AR resulting in increased AR binding at these sites in AIPCa. It is also possible that other active histone marks present on gene enhancers (Barski et al., 2007) may play a role to facilitate transcription factor and coactivator recruitment. Interestingly, while silencing of FoxA1 does not affect AR target genes *PSA* and *TMPRSS2* expression and androgen-induced cell cycle progression in LNCaP cells (Wang et al., 2007), FoxA1 function is required for *UBE2C* expression in abl cells, suggesting that FoxA1 may play a more important role in AIPCa than in ADPCa.

The finding that differential H3K4 marks are required for differential AR binding raises the question of what are the mechanisms responsible for the establishment of the differential histone marks in AIPCa versus ADPCa. It is possible that the expression of H3K4 histone methyltransferases is higher in AIPCa than in ADPCa. Alternatively, it is conceivable that the specific mechanisms for recruiting the enzymes that make these marks exist in AIPCa but not in ADPCa (Kouzarides, 2007; Ruthenburg et al., 2007). Future studies will be needed to address these possibilities.

Our findings that AR selectively and directly up-regulates M-phase genes in AIPCa may explain why maximal androgen blockade that combines AR antagonists with LHRH inhibitors cannot prolong AIPCa patient survival (Group, 2000) as such therapies will only inhibit the ability of androgen-bound AR to promote G1/S transition in ADPCa but cannot prevent un-liganded AR from accelerating M-phase transition in AIPCa. Interestingly, two recent clinical trials have shown that docetaxel, which disrupts mitosis by inhibiting the depolymerization of microtubules, can modestly improve survival of AIPCa patients (Petrylak et al., 2004; Tannock et al., 2004), supporting an important role of M-phase in AIPCa progression.

Among the M-phase regulatory genes controlled by AR in AIPCa we find that UBE2C protein is over-expressed in AIPCa cases. Interestingly, UBE2C has also been found to be over-expressed in breast, lung, ovary, bladder, thyroid and esophageal carcinomas (Lin et al., 2006; Pallante et al., 2005; Wagner et al., 2004), suggesting a general role of UBE2C in accelerating M-phase transition in solid tumors. Importantly, silencing of UBE2C significantly decreases AIPCa growth by arresting G2/M and S phases, providing a potential new target for therapeutic intervention.

EXPERIMENTAL PROCEDURES

Cell lines and Samples

The prostate cancer cell line LNCaP was obtained from the American Type Culture Collection. abl cell line was provided by Zoran Culig (Innsbruck Medical University, Austria) (Culig et al., 1999). C4-2B cell line was obtained from ViroMed Laboratories (Minneapolis, MN). The prostate cancer tissue microarrays that include 44 normal prostate specimens, 98 ADPCa specimens, and 230 AIPCa specimens were obtained from Arul Chinnaiyan (University of Michigan, MI) and Mark Rubin (Cornell University, NY) as previously described (Rubin et al., 2002). One ADPCa tissue and one AIPCa tissue used for tissue ChIP were obtained form Arul Chinnaiyan.

Cell proliferation assay

Cell proliferation was determined using a WST-1 kit (Roche, Indianapolis, IN).

RNA interference

A control siRNA (siControl) and siRNA targeting AR, CDC20, UBE2C, and CDK1 (ON TARGET plus™ siRNA) were purchased from Dharmacon (Dharmacon, Lafayette, CO). A second siAR has been described (Haag et al., 2005). siRNA transfections were performed using Lipofectamine 2000 (Invitrogen, Carlsbad, CA). The siRNA sequences were listed in Table S1.

Gene expression experiments and analyses

Hormone-depleted LNCaP and abl cells were transfected with siControl or siAR and abl cells were treated with 100 nM DHT or vehicle. Seventy-two hours after siRNA transfection or four and sixteen hours after DHT treatment, total RNA was isolated using an RNeasy kit (Qiagen, Valencia, CA). Biological triplicate total RNA was hybridized to Affymetrix human U133 plus 2.0 expression array (Affymetrix, Santa Clara, CA) at the Dana-Farber Cancer Institute (DFCI) Microarray Core Facility. Microarray data have been submitted to the Gene Expression Omnibus (GEO) repository under the accession number GSE11428. The expression raw data for LNCaP cells in the presence or absence of androgen was from our previous work (Wang et al., 2007) (GEO dataset GSE7868). Two clinical ADPCa/AIPCa expression data were retrieved from GSE3325 and obtained from Steve Balk. All gene expression data was normalized and summarized with RMA algorithm (Irizarry et al., 2003) and an updated RefSeq

probe definition (Dai et al., 2005). Significance Analysis of Microarrays (SAM) algorithm (Tusher et al., 2001) was used to detect the differentially expressed genes and calculate the q-values (False Discovery Rate). Genes with q-value less than 0.05 was used to select the differentially expressed genes. Two-way hierarchical clustering analysis was performed to group both gene expression changes (rows) and conditions (columns). Gene Ontology (GO) analysis was performed using the web tool Database for Annotation, Visualization and Integrated Discovery (DAVID) (http://david.abcc.ncifcrf.gov/).

ChIP-on-chip and standard ChIP assays

AR ChIP was performed as previously described (Wang et al., 2007). The ChIP-enriched DNA was amplified, labeled, and hybridized to Affymetrix Human Tiling 2.0R Array Set. Biological triplicate experiments were performed. The ChIP-on-chip raw data are accessible at http://research.dfci.harvard.edu/brownlab/datasets/. ChIPhttp://research.dfci.harvard.edu/brownlab/datasets/. -on-chip data were analyzed using MAT algorithm (Johnson et al., 2006). Antibodies used for ChIP are available in the Supplemental Experimental Procedures.

Correlation of AR binding to gene expression

Genes having AR binding sites within certain distance were defined as those having at least one such site within the distance relative to the transcription start sites. For each category of AR-regulated genes, the percentage of genes having AR binding sites in LNCaP or abl cells within 20–100 kb was calculated. All RefSeq genes in Affymetrix human U133 plus 2.0 expression array were used as the control category. Chi-squared test was used to assess the statistical significance for the percentages of AR-regulated genes having AR binding sites.

Real-time RT-PCR

Real-time RT-PCR was performed as before (Wang et al., 2007). Primers used are listed in Table S1.

Western blots analysis

Western blots were performed as previously described (Wang et al., 2002). Antibodies used are available in the Supplemental Experimental Procedures.

Quantitative chromosome conformation capture assay (3C-qPCR)

3C-qPCR assays were performed essentially as described (Hagege et al., 2007) with minor modifications. Details are available in the Supplemental Experimental Procedures.

Tissue microarray analysis

The immunohistochemistry of UBE2C on tissue microarrays was performed as described (Wang et al., 2008) using anti-UBE2C (A650) at 1:600 dilution. Details are available in the Supplemental Experimental Procedures.

Fluorescence-activated cell sorting (FACS) analysis

siRNA transfected LNCaP and abl cells were collected, stained with propidium iodide and DNA contents were analyzed by DFCI Cytometry Core Facility.

Supplementary Material

Refer to Web version on PubMed Central for supplementary material.

Acknowledgments

This work was supported by grants from Dana-Farber/Harvard Cancer Center prostate SPORE (to M.B), National Institutes of Health (K99 CA126160 to Q.W.) and Department of Defense (W81XWH-07-1-0037 to X.S.L). We thank Drs. Roland Schüle for providing KDM1 constructs and Michael Rape for UBE2C constructs. We also thank Drs. James DeCaprio, Gustavo Leone, Tim Huang, Yun Li, and Shengjun Ren for helpful discussions and Dr. Chunpeng Zhang and Anna Rorick for technical assistance.

References

Barski A, Cuddapah S, Cui K, Roh TY, Schones DE, Wang Z, Wei G, Chepelev I, Zhao K. High-resolution profiling of histone methylations in the human genome. Cell 2007;129:823–837. [PubMed: 17512414]

Bernstein BE, Kamal M, Lindblad-Toh K, Bekiranov S, Bailey DK, Huebert DJ, McMahon S, Karlsson EK, Kulbokas EJ 3rd, Gingeras TR, et al. Genomic maps and comparative analysis of histone modifications in human and mouse. Cell 2005;120:169–181. [PubMed: 15680324]

Carroll JS, Liu XS, Brodsky AS, Li W, Meyer CA, Szary AJ, Eeckhoute J, Shao W, Hestermann EV, Geistlinger TR, et al. Chromosome-wide mapping of estrogen receptor binding reveals long-range regulation requiring the forkhead protein FoxA1. Cell 2005;122:33–43. [PubMed: 16009131]

Chen CD, Welsbie DS, Tran C, Baek SH, Chen R, Vessella R, Rosenfeld MG, Sawyers CL. Molecular determinants of resistance to antiandrogen therapy. Nat Med 2004;10:33–39. [PubMed: 14702632]

Comstock CE, Knudsen KE. The complex role of AR signaling after cytotoxic insult: implications for cell-cycle-based chemotherapeutics. Cell Cycle 2007;6:1307–1313. [PubMed: 17568191]

Culig Z, Hoffmann J, Erdel M, Eder IE, Hobisch A, Hittmair A, Bartsch G, Utermann G, Schneider MR, Parczyk K, et al. Switch from antagonist to agonist of the androgen receptor bicalutamide is associated with prostate tumour progression in a new model system. Br J Cancer 1999;81:242–251. [PubMed: 10496349]

Dai M, Wang P, Boyd AD, Kostov G, Athey B, Jones EG, Bunney WE, Myers RM, Speed TP, Akil H, et al. Evolving gene/transcript definitions significantly alter the interpretation of GeneChip data. Nucleic Acids Res 2005;33:e175. [PubMed: 16284200]

Debes JD, Tindall DJ. Mechanisms of androgen-refractory prostate cancer. N Engl J Med 2004;351:1488–1490. [PubMed: 15470210]

Feldman BJ, Feldman D. The development of androgen-independent prostate cancer. Nat Rev Cancer 2001;1:34–45. [PubMed: 11900250]

Girard F, Strausfeld U, Fernandez A, Lamb NJ. Cyclin A is required for the onset of DNA replication in mammalian fibroblasts. Cell 1991;67:1169–1179. [PubMed: 1836977]

Group PCTC. Maximum androgen blockade in advanced prostate cancer: an overview of the randomised trials. Lancet 2000;355:1491–1498. [PubMed: 10801170]

Haag P, Bektic J, Bartsch G, Klocker H, Eder IE. Androgen receptor down regulation by small interference RNA induces cell growth inhibition in androgen sensitive as well as in androgen independent prostate cancer cells. J Steroid Biochem Mol Biol 2005;96:251–258. [PubMed: 15982869]

Hagege H, Klous P, Braem C, Splinter E, Dekker J, Cathala G, de Laat W, Forne T. Quantitative analysis of chromosome conformation capture assays (3C-qPCR). Nat Protoc 2007;2:1722–1733. [PubMed: 17641637]

Heinlein CA, Chang C. Androgen receptor in prostate cancer. Endocr Rev 2004;25:276–308. [PubMed: 15082523]

Heintzman ND, Stuart RK, Hon G, Fu Y, Ching CW, Hawkins RD, Barrera LO, Van Calcar S, Qu C, Ching KA, et al. Distinct and predictive chromatin signatures of transcriptional promoters and enhancers in the human genome. Nat Genet 2007;39:311–318. [PubMed: 17277777]

Irizarry RA, Hobbs B, Collin F, Beazer-Barclay YD, Antonellis KJ, Scherf U, Speed TP. Exploration, normalization, and summaries of high density oligonucleotide array probe level data. Biostatistics 2003;4:249–264. [PubMed: 12925520]

Johnson DS, Li W, Gordon DB, Bhattacharjee A, Curry B, Ghosh J, Brizuela L, Carroll JS, Brown M, Flicek P, et al. Systematic evaluation of variability in ChIP-chip experiments using predefined DNA targets. Genome Res 2008;18:393–403. [PubMed: 18258921]

Johnson WE, Li W, Meyer CA, Gottardo R, Carroll JS, Brown M, Liu XS. Model-based analysis of tiling-arrays for ChIP-chip. Proc Natl Acad Sci U S A 2006;103:12457–12462. [PubMed: 16895995]

Kouzarides T. Chromatin modifications and their function. Cell 2007;128:693–705. [PubMed: 17320507]

Lin J, Raoof DA, Wang Z, Lin MY, Thomas DG, Greenson JK, Giordano TJ, Orringer MB, Chang AC, Beer DG, et al. Expression and effect of inhibition of the ubiquitin-conjugating enzyme E2C on esophageal adenocarcinoma. Neoplasia 2006;8:1062–1071. [PubMed: 17217624]

Lupien M, Eeckhoute J, Meyer CA, Wang Q, Zhang Y, Li W, Carroll JS, Liu XS, Brown M. FoxA1 translates epigenetic signatures into enhancer-driven lineage-specific transcription. Cell 2008;132:958–970. [PubMed: 18358809]

Mangelsdorf DJ, Thummel C, Beato M, Herrlich P, Schutz G, Umesono K, Blumberg B, Kastner P, Mark M, Chambon P, et al. The nuclear receptor superfamily: the second decade. Cell 1995;83:835–839. [PubMed: 8521507]

Pallante P, Berlingieri MT, Troncone G, Kruhoffer M, Orntoft TF, Viglietto G, Caleo A, Migliaccio I, Decaussin-Petrucci M, Santoro M, et al. UbcH10 overexpression may represent a marker of anaplastic thyroid carcinomas. Br J Cancer 2005;93:464–471. [PubMed: 16106252]

Petrylak DP, Tangen CM, Hussain MH, Lara PN Jr, Jones JA, Taplin ME, Burch PA, Berry D, Moinpour C, Kohli M, et al. Docetaxel and estramustine compared with mitoxantrone and prednisone for advanced refractory prostate cancer. N Engl J Med 2004;351:1513–1520. [PubMed: 15470214]

Prigent C, Dimitrov S. Phosphorylation of serine 10 in histone H3, what for? J Cell Sci 2003;116:3677–3685. [PubMed: 12917355]

Reddy SK, Rape M, Margansky WA, Kirschner MW. Ubiquitination by the anaphase-promoting complex drives spindle checkpoint inactivation. Nature 2007;446:921–925. [PubMed: 17443186]

Resnitzky D, Hengst L, Reed SI. Cyclin A-associated kinase activity is rate limiting for entrance into S phase and is negatively regulated in G1 by p27Kip1. Mol Cell Biol 1995;15:4347–4352. [PubMed: 7623829]

Rubin MA, Zhou M, Dhanasekaran SM, Varambally S, Barrette TR, Sanda MG, Pienta KJ, Ghosh D, Chinnaiyan AM. alpha-Methylacyl coenzyme A racemase as a tissue biomarker for prostate cancer. Jama 2002;287:1662–1670. [PubMed: 11926890]

Ruthenburg AJ, Allis CD, Wysocka J. Methylation of lysine 4 on histone H3: intricacy of writing and reading a single epigenetic mark. Mol Cell 2007;25:15–30. [PubMed: 17218268]

Scher HI, Sawyers CL. Biology of progressive, castration-resistant prostate cancer: directed therapies targeting the androgen-receptor signaling axis. J Clin Oncol 2005;23:8253–8261. [PubMed: 16278481]

Schuur ER, Henderson GA, Kmetec LA, Miller JD, Lamparski HG, Henderson DR. Prostate-specific antigen expression is regulated by an upstream enhancer. J Biol Chem 1996;271:7043–7051. [PubMed: 8636136]

Shang Y, Myers M, Brown M. Formation of the androgen receptor transcription complex. Mol Cell 2002;9:601–610. [PubMed: 11931767]

Shao W, Keeton EK, McDonnell DP, Brown M. Coactivator AIB1 links estrogen receptor transcriptional activity and stability. Proc Natl Acad Sci U S A 2004;101:11599–11604. [PubMed: 15289619]

Shi Y, Lan F, Matson C, Mulligan P, Whetstine JR, Cole PA, Casero RA. Histone demethylation mediated by the nuclear amine oxidase homolog LSD1. Cell 2004;119:941–953. [PubMed: 15620353]

Stanbrough M, Bubley GJ, Ross K, Golub TR, Rubin MA, Penning TM, Febbo PG, Balk SP. Increased expression of genes converting adrenal androgens to testosterone in androgen-independent prostate cancer. Cancer Res 2006;66:2815–2825. [PubMed: 16510604]

Sun Z, Pan J, Balk SP. Androgen receptor-associated protein complex binds upstream of the androgen-responsive elements in the promoters of human prostate-specific antigen and kallikrein 2 genes. Nucleic Acids Res 1997;25:3318–3325. [PubMed: 9241247]

Tannock IF, de Wit R, Berry WR, Horti J, Pluzanska A, Chi KN, Oudard S, Theodore C, James ND, Turesson I, et al. Docetaxel plus prednisone or mitoxantrone plus prednisone for advanced prostate cancer. N Engl J Med 2004;351:1502–1512. [PubMed: 15470213]

Thalmann GN, Sikes RA, Wu TT, Degeorges A, Chang SM, Ozen M, Pathak S, Chung LW. LNCaP progression model of human prostate cancer: androgen-independence and osseous metastasis. Prostate 2000;44:91–103. [PubMed: 10881018]Jul 101; 144(102)

Tomlins SA, Mehra R, Rhodes DR, Cao X, Wang L, Dhanasekaran SM, Kalyana-Sundaram S, Wei JT, Rubin MA, Pienta KJ, et al. Integrative molecular concept modeling of prostate cancer progression. Nat Genet 2007;39:41–51. [PubMed: 17173048]

Tusher VG, Tibshirani R, Chu G. Significance analysis of microarrays applied to the ionizing radiation response. Proc Natl Acad Sci U S A 2001;98:5116–5121. [PubMed: 11309499]

Varambally S, Yu J, Laxman B, Rhodes DR, Mehra R, Tomlins SA, Shah RB, Chandran U, Monzon FA, Becich MJ, et al. Integrative genomic and proteomic analysis of prostate cancer reveals signatures of metastatic progression. Cancer Cell 2005;8:393–406. [PubMed: 16286247]

Wagner KW, Sapinoso LM, El-Rifai W, Frierson HF, Butz N, Mestan J, Hofmann F, Deveraux QL, Hampton GM. Overexpression, genomic amplification and therapeutic potential of inhibiting the UbcH10 ubiquitin conjugase in human carcinomas of diverse anatomic origin. Oncogene 2004;23:6621–6629. [PubMed: 15208666]

Wang H, Leav I, Ibaragi S, Wegner M, Hu GF, Lu ML, Balk SP, Yuan X. SOX9 is expressed in human fetal prostate epithelium and enhances prostate cancer invasion. Cancer Res 2008;68:1625–1630. [PubMed: 18339840]

Wang Q, Carroll JS, Brown M. Spatial and temporal recruitment of androgen receptor and its coactivators involves chromosomal looping and polymerase tracking. Mol Cell 2005;19:631–642. [PubMed: 16137620]

Wang Q, Li W, Liu XS, Carroll JS, Janne OA, Keeton EK, Chinnaiyan AM, Pienta KJ, Brown M. A hierarchical network of transcription factors governs androgen receptor-dependent prostate cancer growth. Mol Cell 2007;27:380–392. [PubMed: 17679089]

Wang Q, Sharma D, Ren Y, Fondell JD. A coregulatory role for the TRAP-mediator complex in androgen receptor-mediated gene expression. J Biol Chem 2002;277:42852–42858. [PubMed: 12218053]

Xu Y, Chen SY, Ross KN, Balk SP. Androgens induce prostate cancer cell proliferation through mammalian target of rapamycin activation and post-transcriptional increases in cyclin D proteins. Cancer Res 2006;66:7783–7792. [PubMed: 16885382]

Yu DC, Sakamoto GT, Henderson DR. Identification of the transcriptional regulatory sequences of human kallikrein 2 and their use in the construction of calydon virus 764, an attenuated replication competent adenovirus for prostate cancer therapy. Cancer Res 1999;59:1498–1504. [PubMed: 10197620]

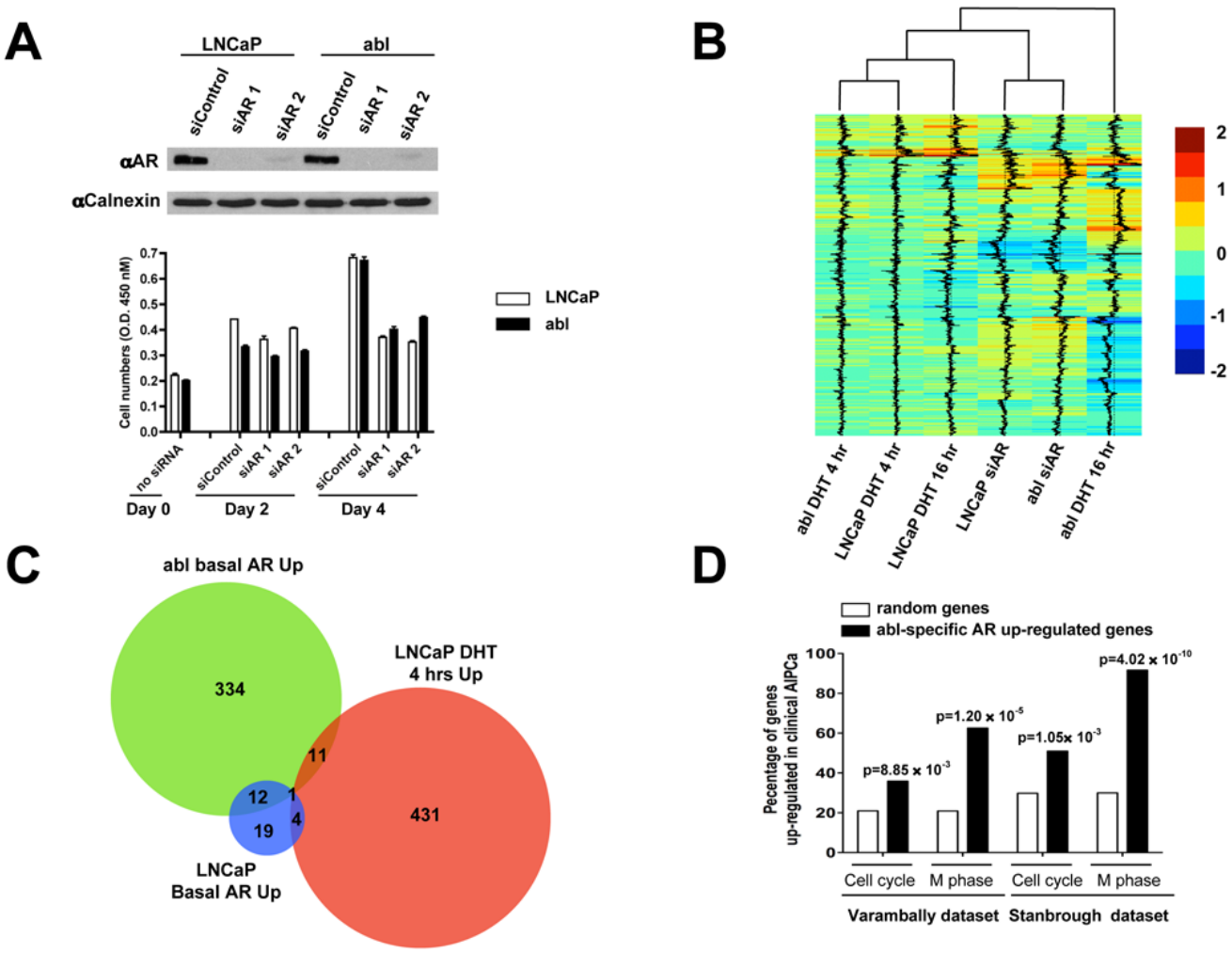

Figure 1. AR silencing in abl cells significantly decreases M phase cell cycle gene expression

(A) AR silencing decreases both LNCaP and abl cell proliferation. LNCaP cells were cultured regular RPMI 1640 supplemented with 10% fetal bovine serum (FBS). abl cells were grown in phenol-red free RPMI 1640 supplemented with 10% charcoal/dextran-stripped FBS. Both cell lines were grown in the absence of supplemental DHT. Cells were transfected with two independent AR siRNA. The cell proliferation was measured on day 2 and day 4 after siRNA transfection using the WST-1 assay (mean (n=3)±s.e.).

(B) Cluster analysis of genes differentially expressed ($q<0.05$) by either DHT treatment and/or siAR transfection. Unsupervised hierarchical clustering of genes (rows) from cells in different conditions (columns) was performed. Brown and blue color represents up-regulation and down-regulation, respectively.

(C) A Venn diagram showing the basal AR up-regulated genes in LNCaP and abl cells and DHT 4 hr up-regulated genes in LNCaP cells.

(D) Comparison of abl-specific AR up-regulated genes with up-regulated genes in two clinical AIPCa datasets (Stanbrough et al., 2006; Varambally et al., 2005).

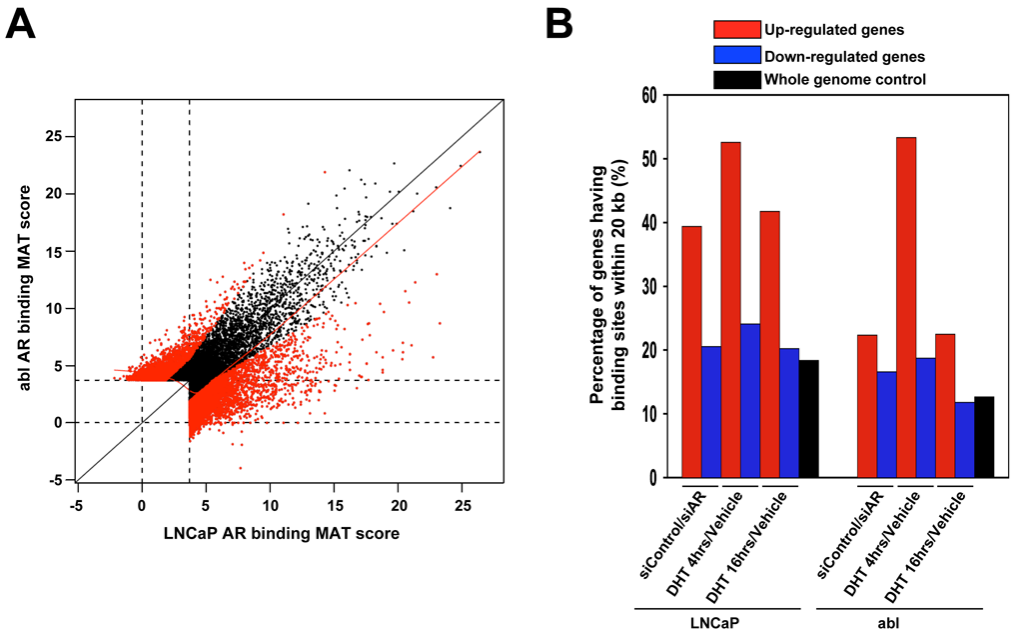

Figure 2. AR directly regulates basal and activated AR up-regulated genes in LNCaP and abl cells

(A) Comparison of AR whole genome binding in LNCaP and abl cells. Triplicate AR whole genome ChIP-on-chip was performed in LNCaP and abl cells treated with DHT for 4 hr. MAT was used to detect AR ChIP-enriched regions. Each dot represents a binding site. Red dots represents differential binding while dark dots refers to non-differential binding.

(B) Correlation of AR binding to differential gene expression in LNCaP and abl cells. The graph represents the percentage of genes having AR binding sites with 20 kb of the transcription start sites. The enrichment of AR binding near the TSS of up-regulated genes over whole genome background is statistically significant in both LNCaP and abl cells (Chi-squared test, LNCaP (siControl/siAR, $p=1.82 \times 10^{-3}$; DHT 4 hrs/vehicle, $p=2.58 \times 10^{-71}$; DHT 16 hrs/vehicle, $p=9.57 \times 10^{-65}$), abl (siControl/siAR, $p=6.90 \times 10^{-8}$; DHT 4 hrs/vehicle, $p=7.91 \times 10^{-46}$; DHT 16 hrs/vehicle, $p=2.06 \times 10^{-27}$).

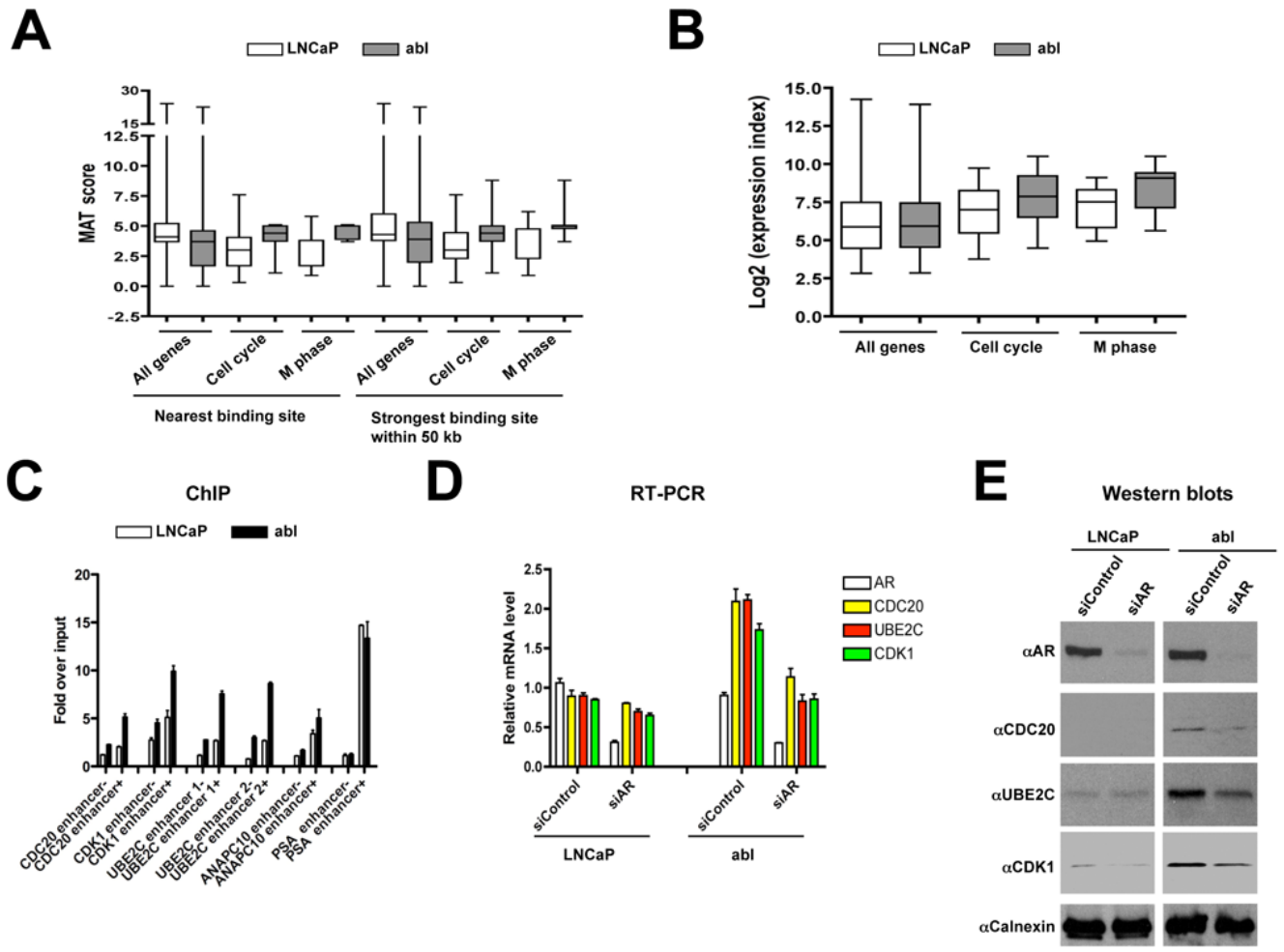

Figure 3. Higher occupancy of AR binding near the M-phase cell cycle genes leads to higher expression levels of these genes in abl cells

(A) Comparison of MAT score of the nearest and the strongest AR binding site within 50 kb of all genes, basal AR up-regulated cell cycle genes and M phase genes in LNCaP and abl cells. The difference of all genes and M-phase genes between two cell lines is statistically significant (t-test on two independent samples, means+s.e., nearest binding site (all genes, abl/LNCaP=0.78-fold, $p=2.17 \times 10^{-154}$, M-phase genes, abl/LNCaP= 1.75-fold, $p=5.85 \times 10^{-4}$), strongest binding site (all genes, abl/LNCaP=0.8-fold, $p=2.48\times 10^{-127}$, M-phase genes, abl/LNCaP= 1.64-fold, $p=6.29 \times 10^{-3}$).

(B) Comparison of gene expression index of all genes, basal AR up-regulated cell cycle and M-phase genes in abl cells. Significant difference is observed between cell cycle and M-phase gene expression in two cell lines (t-test on two independent samples, means+s.e., cell cycle, 1.13-fold, $p=4.51 \times 10^{-3}$, M-phase 1.18-fold, $p=2.65 \times 10^{-3}$).

(C) ChIP analysis of AR recruitment to various AR binding sites near cell cycle genes. The PSA enhancer was used as a positive control. ChIP assays were performed with anti-AR antibodies in the presence (+) and absence (−) of DHT. (mean (n=2)±s.e.).

(D) AR silencing specifically decrease high expression of M phase genes *CDC20*, *UBE2C* and *CDK1* in abl cells. Seventy-two hours after siRNA transfection into LNCaP and abl cells in the absence of DHT, total RNA was isolated and amplified by real-time RT-PCR using gene specific primers (mean (n=3) ±s.e.).

(E) AR silencing specifically decreases high protein expression levels of CDC20, UBE2C and CDK1 in abl cells. Western blots were performed using the antibodies indicated ninety-six hours after siRNA transfection into LNCaP and abl cells without DHT.

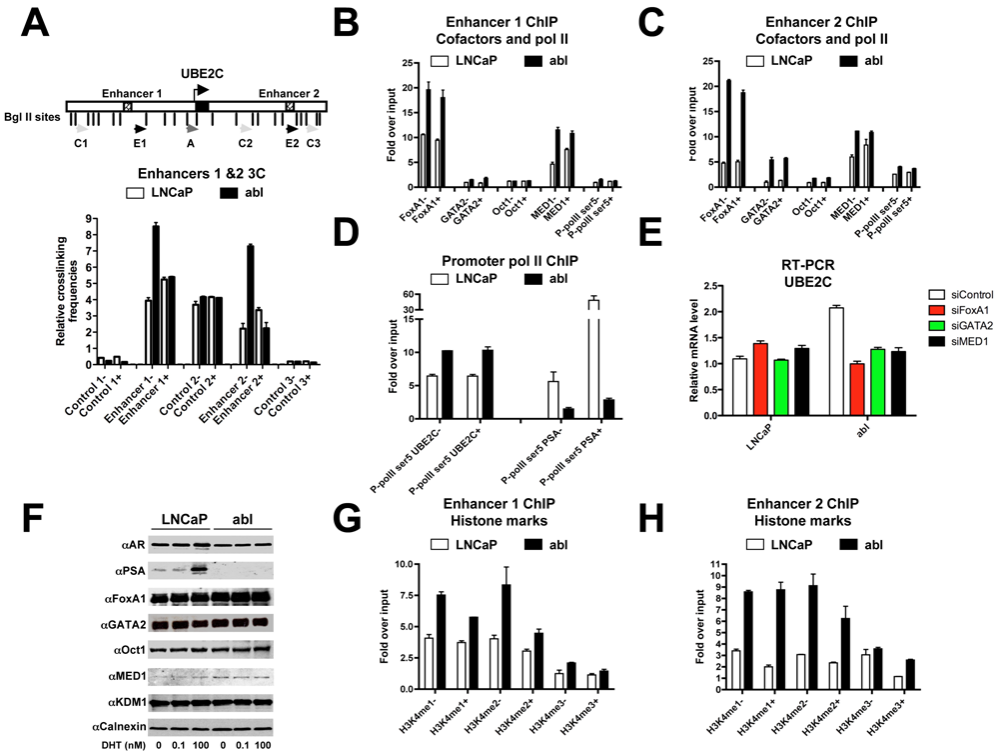

Figure 4. Higher levels of active epigenetic histone marks and recruitment of collaborating factors are correlated with greater AR occupancy on the UBE2C enhancers in abl cells

(A)

Upper panel: Schematic diagram showing the UBE2C locus. The arrows indicate the location and the direction of primers used in the 3C-qPCR assays. The anchor primer [A] and the Taqman probe were designed in the Bgl II fragment containing the UBE2C promoter. All other test primers [C1, C2, C3, E1, and E2] were designed within 50 bp to the restriction sites.

Lower panel: The two UBE2C enhancers interact with the UBE2C promoter in abl cells. 3C assays were performed using Bgl II enzyme in LNCaP and abl cells in the presence (+) and absence (−) of DHT (mean (n=2) ±s.e.).

(B and C) Stronger FoxA1 and MED1 binding to the UBE2C enhancer 1 and FoxA1, GATA2 and MED1 binding to the UBE2C enhancer 2 in abl cells than in LNCaP cells. ChIP assays were performed using antibodies against FoxA1, GATA2, Oct1, MED1 and P-pol II ser 5 in LNCaP and abl cells treated with (+) and without (−) androgen (mean (n=2) ±s.e.).

(D) Higher p-pol II ser 5 occupancy on the UBE2C promoter in abl cells than in LNCaP cells. P-pol II ser 5 binding at the PSA promoter was served as a control. ChIP assays were conducted in LNCaP and abl cells in the presence (+) and absence (−) of DHT using an anti-p-pol II ser 5 antibody.

(E) Effects of siRNA on UBE2C gene expression in LNCaP and abl cells. Real-time PCR was performed seventy-two hours after siRNA transfection in the absence of DHT (mean (n=3) ±s.e.).

(F) Comparison of protein expression in LNCaP and abl cells by Western blots. Western blots analyses were performed comparing AR, PSA, FoxA1, GATA2, Oct1, MED1 and KDM1 protein expression levels in the absence and presence of DHT (0.1 nM and 100 nM).

(G and H) UBE2C enhancers 1 (G) and 2 (H) have higher H3K4me1 and H3K4me2 levels in abl cells than in LNCaP cells. Levels of H3K4 me1, H3K4me2 and H3K4me3 on UBE2C

enhancers were determined by ChIP assays in the presence (+) and absence (−) of DHT using specific antibodies against H3K4 me1, H3K4me2 and H3K4me3 (mean (n=2) ±s.e.).

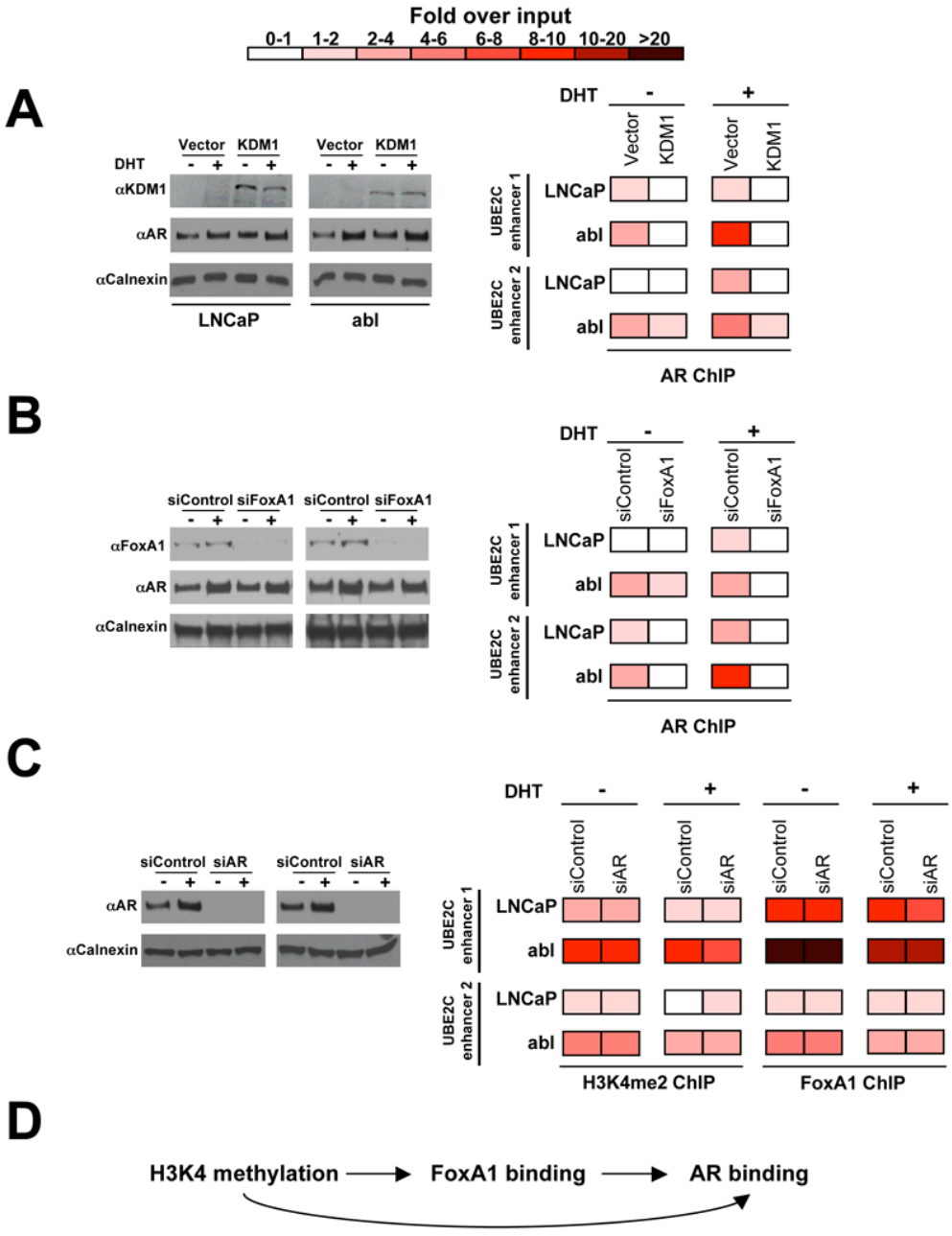

Figure 5. H3K4me2 and FoxA1 act upstream of AR and are required for differential AR binding in abl cells

(A) Over-expression of KDM1 abolishes differential AR binding in LNCaP and abl cells. Cells were transfected with a FLAG-tagged KDM1 vector or an empty vector control. Three days after transfection, cells were treated with (+) or without (−) DHT. AR ChIP was then performed on the UBE2C enhancers. The over-expression of KDM1 levels was monitored by Western blot.

(B) FoxA1 silencing abolishes differential AR binding in LNCaP and abl cells. Cells were transfected with siFoxA1. AR ChIP was then performed in the presence (+) and absence (−) of DHT on the UBE2C enhancers. The reduction of FoxA1 protein level was verified by Western blot.

(C) AR silencing has no effect on differential H3K4me2 level and FoxA1 recruitment. Cells were transfected with siAR. H3K4me2 and FoxA1 ChIP were then performed in the presence (+) and absence (−) of DHT on the UBE2C enhancers. The reduction of AR protein was demonstrated by Western blot.

D) A hierarchical model for AR action on the UBE2C enhancers. H3K4 methylation and FoxA1 act upstream of AR, and H3K4 methylation functions upstream of FoxA1.

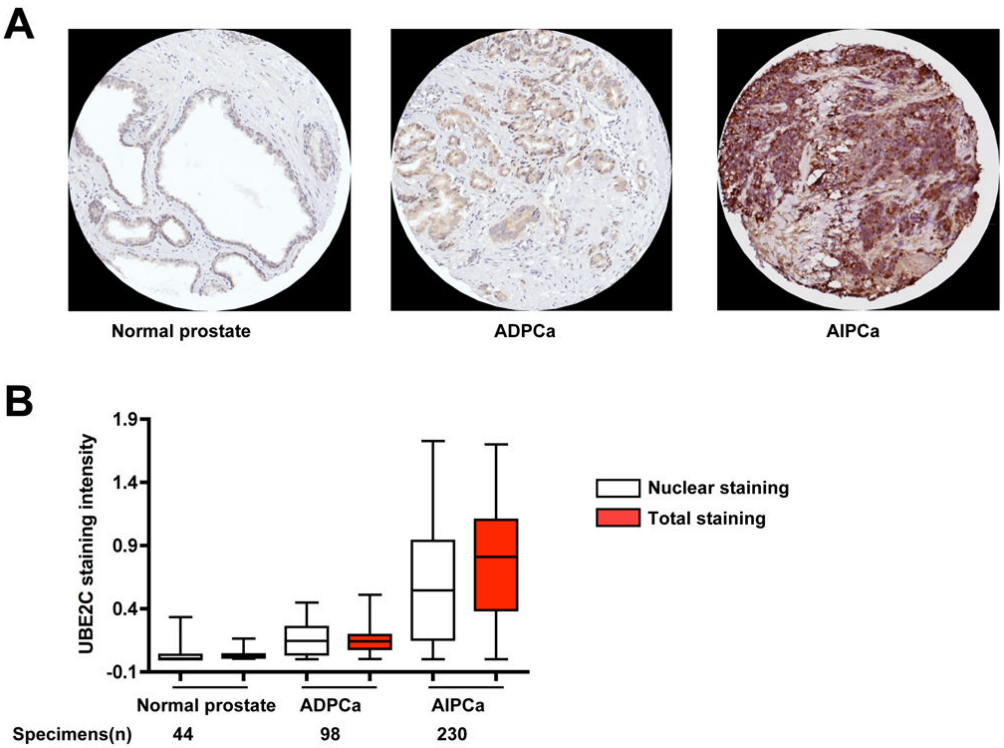

Figure 6. UBE2C protein expression level is over-expressed in AIPCa cases

(A) Representative tissue microarray elements stained with an antibody against UBE2C (magnification 20 ×). Stronger staining of UBE2C was seen in AIPCa than in ADPCa.

(B) Analysis of UBE2C protein expression in normal prostate, ADPCa and AIPCa. Tissue microarrays were scanned and scored using the Ariol image analysis system. Nuclear staining and total staining reflect a combination of the percentage of positive nuclei and the intensity of the stain, and a combination of the positive area score and the intensity of the stain, respectively. AIPCa has stronger nuclear staining and total staining\\than ADPCa (Welch one-side t-test, $p< 2.2 \times 10^{-16}$ for both staining scores). ADPCa has higher nuclear staining and total staining scores compared with normal prostate ($p=5.80 \times 10^{-13}$, $p< 2.2 \times 10^{-16}$, respectively).

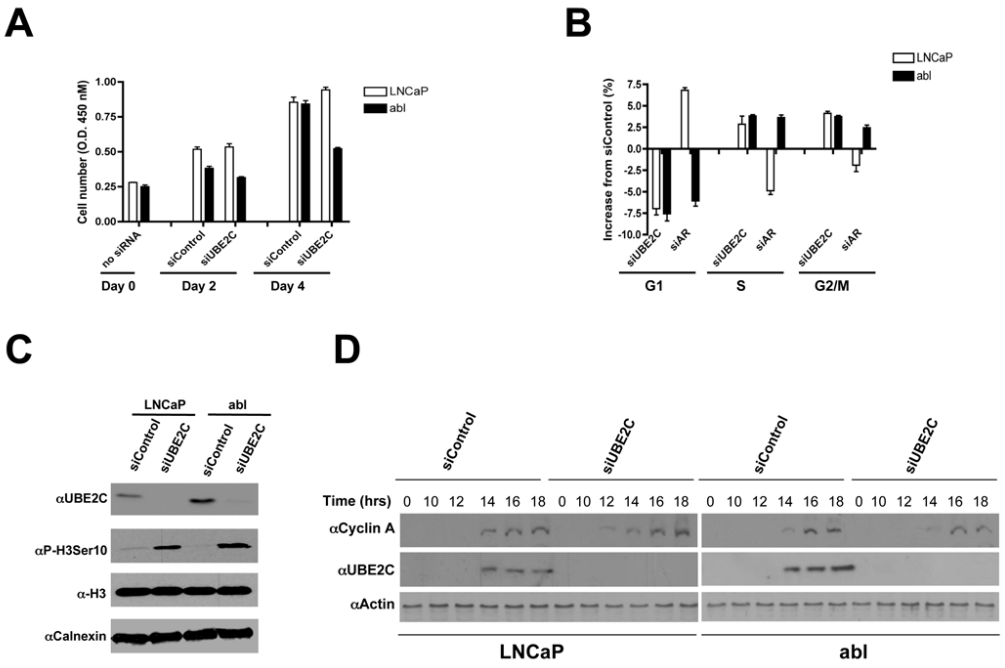

Figure 7. UBE2C silencing selectively decreases abl cell growth

(A) Silencing of UBE2C selectively decreases abl cell proliferation. LNCaP and abl were plated as described in Figure 1.The cell proliferation was measured on day 2 and day 4 after siRNA transfection using the WST-1 assay (mean (n=3)±s.e.).

(B) Silencing of UBE2C increases G2/M and S phase cells in LNCaP and abl cells. Ninety-six hr after siRNAs transfection in the absence of DHT, cells were analyzed by FACS (mean (n=2) ±s.e.).

(C) Silencing of UBE2C leads to a prolonged mitosis as indicated by P-H3Ser10. Ninety-six hr post siRNAs transfection in the absence of DHT, Western blots were performed with histone extraction (for P-H3Ser10 and total H3) or whole cell lysate (for UBE2C and calnexin) using the antibodies indicated.

(D) UBE2C silencing results in a shortened G1 in LNCaP cells but not in abl cells. LNCaP and abl cells were transfected with siControl or siUBE2C in the absence of DHT. After 6–8 hr, cells were synchronized in G0 by serum starvation for 24 hr. Cells were stimulated to re-enter cell cycle by the addition of 20% serum and harvested at the indicated time points. Cell lysates were subjected to Western blot with the indicated antibodies.